Neuroscience 129 (2004) 703–718

CALCIUM INFLUX THROUGH PRESYNAPTIC 5-HT$_3$ RECEPTORS FACILITATES GABA RELEASE IN THE HIPPOCAMPUS: *IN VITRO* SLICE AND SYNAPTOSOME STUDIES

T. J. TURNER,[a] D. J. MOKLER[b,c] AND J. I. LUEBKE[c,d]*

[a]*Department of Neuroscience, Tufts University School of Medicine, Boston, MA 02111, USA*

[b]*Department of Pharmacology, University of New England College of Osteopathic Medicine, Biddeford, ME 04005, USA*

[c]*Center for Behavioral Development, Department of Psychiatry, M923, Boston University School of Medicine, 85 East Newton Street, Boston, MA 02118, USA*

[d]*Department of Anatomy and Neurobiology, Boston University School of Medicine, 715 Albany Street, Boston, MA 02118, USA*

Abstract—Serotonin 5-hydroxytryptamine type 3 receptors (5HT$_3$R) are Ca^{2+}-permeant, non-selective cation channels that have been localized to presynaptic terminals and demonstrated to modulate neurotransmitter release. In the present study the effect of 5-HT on GABA release in the hippocampus was characterized using both electrophysiological and biochemical techniques. 5-HT elicited a burst-like, 6- to 10-fold increase in the frequency of GABA$_A$ receptor-mediated inhibitory postsynaptic currents (IPSCs) measured with whole-cell voltage-clamp recordings of CA1 neurons in hippocampal slices. When tetrodotoxin was used to block action potential propagation, the 5-HT-induced burst of IPSCs was still observed. Stimulation of hippocampal synaptosomes with 5-HT resulted in a significant increase in the amount of [^{3}H]GABA released by hyperosmotic saline. In both preparations, the 5-HT effect was shown to be mediated by 5HT$_3$Rs, as it was mimicked by the selective 5HT$_3$R agonist *m*-chlorophenyl biguanide and blocked by the selective 5HT$_3$R antagonist 3-tropanylindole-3-carboxylate hydrochloride. The 5HT$_3$R-mediated increase in GABA release was blocked by 100 μM cadmium or by omitting Ca^{2+} in external solutions, indicating the Ca^{2+}-dependence of the effect. The high voltage-activated Ca^{2+} channel blockers ω-conotoxin GVIA and ω-conotoxin MVIIC and 10 μM cadmium had no significant effect on the 5-HT$_3$R-mediated enhancement of GABA release, indicating that Ca^{2+} influx through the 5-HT$_3$R facilitates GABA release. Taken together, these data provide direct evidence that Ca^{2+} entry via presynaptic 5HT$_3$Rs facilitates the release of GABA from hippocampal interneurons.

*Correspondence to: J. I. Luebke, Center for Behavioral Development, M923, Boston University School of Medicine, 85 East Newton Street, Boston, MA 02118, USA. Tel: +1-617-638-4930; fax: +1-617-638-5890.
E-mail address: jluebke@bu.edu (J. I. Luebke).

Abbreviations: CNQX, 6-cyano-7-nitroquinoxaline-2,3-dione; D-AP5, D-2-amino-5-phosphonovaleric acid; HVA, high voltage-activated; ICS-205, 930, 3-tropanylindole-3-carboxylate hydrochloride; IPSC, inhibitory postsynaptic current; K-S, Kolmogorov-Smirnov; *m*-CPBG, *m*-chlorophenyl biguanide; mIPSC, minature inhibitory postsynaptic current; RP, releasable pools; TTx, tetrodotoxin; 5-HT, 5-hydroxytryptamine; 5-HT$_3$R, 5-hydroxytryptamine$_3$ receptor.

Key words: whole-cell patch-clamp, hippocampal slice, synaptosome, serotonin, GABA$_A$ receptor, miniature inhibitory postsynaptic currents.

Inhibition of principal cells by GABAergic interneurons plays a critical role in the regulation of information flow through the hippocampus (review, Freund and Buzsáki, 1996). The activity of inhibitory interneurons in the hippocampus is modulated by a number of inputs from subcortical monoaminergic nuclei, including the serotonergic midbrain raphe nuclei (Miettinen and Freund, 1992a,b; Acsády et al., 1993; Papp et al., 1999; Gulyás et al., 1999). 5-Hydroxytryptamine (5-HT) produces diverse physiological actions in hippocampal neurons by activating a heterogeneous population of 5-HT receptors (Andrade, 1998; Barnes and Sharp, 1999). The 5-HT$_3$ receptor (5HT$_3$R) is unique among these receptors in that it belongs to the superfamily of ligand-gated ionotropic receptors. 5HT$_3$Rs mediate a rapidly activating, desensitizing, inward current carried by sodium and potassium ions that is very similar to nicotinic acetylcholine receptors and other ligand-gated ionotropic receptors (Derkach et al., 1989; Yakel and Jackson, 1988; Maricq et al., 1991).

5HT$_3$Rs are present on presynaptic nerve terminals (Waeber et al., 1988; Laporte et al., 1992; Nichols and Mollard, 1996; Nayak et al., 1999; Katsurabayashi et al., 2003) where they have been shown to have a high Ca^{2+} permeability (Nichols and Mollard, 1996; Ronde and Nichols, 1998; Nayak et al., 1999). These findings suggest a role for the 5HT$_3$R in the presynaptic regulation of neurotransmitter release. Indeed, 5HT$_3$R activation has been shown to enhance the release of a variety of neurotransmitters, including dopamine (Blandina et al., 1989; Chen et al., 1991), cholecystokinin (Paudice and Raiteri, 1991) and GABA (Ropert and Guy, 1991; Piguet and Galvan, 1994; Koyama et al., 2000, 2002; Katsurabayashi et al., 2003). About 50% of hippocampal interneurons express 5HT$_3$Rs (Miettinen and Freund, 1992a,b; Acsády et al., 1993; Papp et al., 1999; Morales and Bloom, 1997), and these interneurons are depolarized by 5-HT$_3$R agonists (Kawa, 1994; McMahon and Kauer, 1997). Intracellular current clamp recordings from *in vitro* slices have shown that 5-HT produces a burst-like increase in the frequency and amplitude of spontaneous inhibitory postsynaptic currents (IPSPs) in rat CA1 pyramidal cells (Ropert and Guy, 1991; Shen and Andrade, 1998) and dentate gyrus granule cells (Piguet and Galvan, 1994), effects that are mimicked by 5-HT$_3$R-selective agonists and blocked by the 5HT$_3$R antagonist

0306-4522/04$30.00+0.00 © 2004 IBRO. Published by Elsevier Ltd. All rights reserved.
doi:10.1016/j.neuroscience.2004.08.020

ICS-205-930. Because this effect was blocked by the sodium-dependent action potential blocker tetrodotoxin (TTx), it was concluded that the increase in the frequency of inhibitory synaptic events elicited by 5-HT was due to the direct depolarization of GABAergic interneurons by 5-HT_3R activation. Thus these studies did not provide insight into the functional relevance of Ca^{2+} permeable 5-HT_3R located on presynaptic terminals. More recently, Katsurabayashi et al. (2003) have provided indirect evidence for a presynaptic locus of action of 5-HT on 5-HT_3Rs using paired-pulse paradigms in hippocampal slices.

A TTx-*resistant* modulation of GABA release by 5-HT_3Rs in mechanically dissociated basolateral amygdala (Koyama et al., 2000, 2002) and CA1 pyramidal (Katsurabayashi et al., 2003) neurons has been demonstrated. In basolateral amygdala neurons, increased GABA release has been shown to be due to calcium influx directly through presynaptic 5-HT_3Rs (Koyama et al., 2000). The mechanism of the 5-HT_3R-mediated increase in GABA release in the hippocampus has not yet been examined. The reason for the discrepancy in findings between previous *in vitro* slice and isolated neuron preparations is not known. Indeed, as noted by Katsurabayashi et al. (2003) definitive evidence that presynaptic 5-HT_3Rs directly mediate GABA release from interneurons in *in vitro* slices has been lacking.

In an effort to address the question of whether presynaptic 5-HT_3R activation results in increased GABA release in *in vitro* hippocampal slices, and to examine the mechanism by which such facilitation occurs, we investigated the actions of 5-HT on IPSCs in CA1 neurons in the hippocampal slice preparation and on [^{3}H]GABA release from hippocampal synaptosomes. We found that 5-HT elicited a burst-like increase in the frequency and amplitude of TTx *resistant* miniature (m)IPSCs in the slice which was mimicked by the 5-HT_3R agonist mCPBG. 5-HT also produced a significant increase in the release of GABA from hippocampal synaptosomes. In this study we characterized these actions and provide further direct evidence, in agreement with the work of Koyama and coworkers (Koyama et al., 2000), for a presynaptic, calcium-dependent role of the 5HT_3R in the facilitation of GABA release.

EXPERIMENTAL PROCEDURES

Preparation of slices

Slices were prepared from juvenile rats as described previously (St. John et al., 1997; Luebke et al., 1993, 2000). Rats were housed at the Boston University Laboratory Animal Science Center (LASC) in strict accordance with animal care guidelines as outlined in the NIH *Guide for the Care and Use of Laboratory Animals* and the U.S. *Public Health Service Policy on Humane Care and Use of Laboratory Animals*. The Boston University LASC is fully accredited by the Association for Assessment and Accreditation of Laboratory Animal Care and all procedures were approved by the Institutional Animal Care and Use Committees of Boston University. Every effort was made to minimize the number of animals used and their suffering. Briefly, 21–30 day old Sprague–Dawley rats were decapitated and the brain rapidly removed into ice-cold oxygenated (95% O_2, 5% CO_2) Ringers solution (concentrations, in mM: 26 $NaHCO_3$, 124 NaCl, 2 KCl, 10 glucose, 3 KH_2PO_4, 2.5 $CaCl_2$, 1.3 $MgCl_2$; pH=7.4; chemicals from Fluka, NY, USA). The hippocampus was dissected from the brain, glued against an agar slab in a tissue holder with cyanoacrylate glue, and placed on the stage of a vibrating microtome in ice-cold oxygenated Ringers solution. Five hundred micron thick transverse sections were cut and placed in a holding chamber containing room temperature, oxygenated Ringers solution. Slices were equilibrated at room temperature in oxygenated Ringers for a minimum of 1 h after which a single slice was positioned in a submersion type slice recording chamber (Harvard Apparatus, Holliston, MA, USA). During experiments, slices were constantly superfused at a flow rate of approximately 2 ml per minute with oxygenated Ringers. Experiments were performed at room temperature (26±1 °C). The results presented are based on stable, long-term recordings from 162 CA1 pyramidal cells.

Whole cell patch clamp recordings

Standard tight-seal, whole cell recordings (Edwards et al., 1989; Luebke et al., 1992, 2000; St. John et al., 1997) were made with patch pipettes fabricated on a Flaming and Brown horizontal micropipette puller (Model P-87; Sutter Instrument Co., Novato, CA, USA) from microhematocrit capillary tubes (Fisher, Pittsburgh, PA, USA). Pipettes were filled with an internal solution of the following composition (in mM): 140 cesium chloride, 2 $MgCl_2$, 0.5 EGTA, and 10 Na-HEPES (pH adjusted to 7.2 with CsOH; chemicals from Fluka). With this internal solution, recording electrodes had resistances of 4–5 MΩ in the external (Ringers) solution. Patch pipettes were lowered 100–200 μm into the CA1 pyramidal cell layer of the slice; when pressure was released a several-hundred MΩ seal was usually obtained. Application of gentle suction resulted in the formation of a GΩ seal, and when suction was increased, whole-cell access was usually achieved. The membrane potential of the cells dropped to the chloride equilibrium potential (0 mV) within 1 min of obtaining whole cell access. Access resistance was measured from responses to small hyperpolarizing and depolarizing current pulses and was checked every few minutes during the course of all experiments. Voltage clamp recordings were performed with List EPC-7 and EPC-9 patch clamp amplifiers (70–90% series resistance compensation) and "Pulse" acquisition software from HEKA Elektronik (Lambrecht, GDR) with Power Mac computers.

Electrophysiological analyses of drug effects on spontaneous IPSCs and mIPSCs

All recordings were performed first in control Ringers solution, prior to the addition of pharmacologic agents. Once stable recording of a cell was obtained, spontaneous IPSCs were recorded in the voltage clamp mode at a holding potential of −80 mV. This hyperpolarized holding potential was used to increase the driving force on Cl^- and thus maximize the amplitude of IPSCs. Baseline spontaneous IPSC data were acquired for a period of 5 min in each cell. In initial experiments, following acquisition of baseline data, 5-HT (10–100 μM) was bath applied to the slice and data acquired for an additional 5 min to determine the effects of 5-HT on spontaneous IPSCs. In subsequent experiments on mIPSCs, baseline spontaneous IPSC data were acquired for 5 min after which the control Ringers solution was switched to Ringers solution that allowed the examination of mIPSCs in isolation from action potential-dependent IPSCs. This solution was composed of control Ringers with the following drugs added: 600 nM TTx (to block action potentials), 10 μM 6-cyano-7-nitroquinoxaline-2,3-dione (CNQX; to block glutamatergic AMPA responses) and 40 μM D-2-amino-5-phosphonovaleric acid (D-AP5; to block glutamatergic NMDA responses). Following collection of baseline mIPSC data for 5 min, 5-HT (10–100 μM) or the 5-HT_3R agonist *m*-chlorophenyl biguanide (*m*-CPBG; 0.1–10 μM) was applied either via the perfusate or locally via a pressure pipette and data

acquired for a further 5 min. In other experiments, 5-HT or *m*-CPBG was applied while the slice was continually perfused with Ringers containing the specific 5-HT_3R antagonist 3-tropanylindole-3-carboxylate hydrochloride (ICS-205,930; 2 nM). In some experiments, the $GABA_A$ receptor antagonist bicuculline methiodide (5 μM) was applied via the perfusate. Finally, the calcium dependence of the 5-HT mediated response was examined by comparing the response to 5-HT elicited in each of the following extracellular solutions: control Ringers (2.5 mM calcium), low (15 μM) calcium, and 0 calcium. The low calcium Ringers solution was prepared by adding 15 μM calcium chloride to the 0 calcium Ringers solution (concentrations, in mM: 26 $NaHCO_3$, 124 NaCl, 2 KCl, 10 glucose, 3 KH_2PO_4, 3.8 $MgCl_2$; pH=7.4; chemicals from Fluka). The 0 Ca^{2+} solution also contained the Ca^{2+} chelator EGTA (2 mM). Ca^{2+} concentration was confirmed with the use of Ca^{2+} selective microelectrode measurements. The measured value for Ca^{2+} was <10 nM for the "0" Ca^{2+} solution. Ten micromolar and 100 μM cadmium solutions were prepared by serial dilution of 1 mM cadmium chloride in phosphate and bicarbonate-free Ringers solution (concentrations, in mM: 26 HEPES, 124 NaCl, 5 KCl, 10 glucose, 2.5 $CaCl_2$, 1.3 $MgCl_2$; pH=7.4; chemicals from Fluka). All drugs were obtained from Sigma/RBI (St. Louis, MO, USA), were prepared as stock solutions, and diluted immediately prior to use.

Preparation of synaptosomes

Synaptosomes were prepared from adult mice as described in detail previously (Turner et al., 1989, 1995a,b). Mice were housed at the Tufts University Laboratory Animal Science Center (LASC) in strict accordance with animal care guidelines as outlined in the NIH *Guide for the Care and Use of Laboratory Animals* and the U.S. *Public Health Service Policy on Humane Care and Use of Laboratory Animals*. The Tufts University LASC is fully accredited by the Association for Assessment and Accreditation of Laboratory Animal Care and all procedures were approved by the Institutional Animal Care and Use Committees of Tufts University.

Hippocampal tissue from adult mice (15–30 g) was dissected and homogenized in 4 ml 0.32 M sucrose, 1 mM EDTA in a "AA" Wheaton glass–Teflon homogenizer (Thomas Scientific). The supernatant fraction remaining after low speed centrifugation (1500×*g*, 10 min) was divided into two equal portions and applied to two identical discontinuous Percoll (Pharmacia) gradients that were centrifuged at 50,000×*g* for 7 min (Dunkley et al., 1988). The material that migrated to the 10/15 and 15/23% Percoll boundaries was collected and washed in basal buffer (145 mM NaCl, 2.7 mM KCl, 1.0 mM $CaCl_2$, 1.0 mM $MgCl_2$, 10 mM glucose, 10 mM HEPES–Tris, pH 7.4) by two 10 min centrifugation steps at 12,000×*g*. The final pellet was resuspended in basal buffer and stored on ice until use.

To initiate [^{3}H]GABA loading, a 45 μl portion of the synaptosomal suspension containing approximately 50 μg of protein was combined with 5 μl of [^{3}H]GABA (27.6 Ci/mMol; Perkin-Elmer Life Sciences, Boston, MA, USA) that had been prepared by evaporating the aqueous stock solution (0.01 N HCl) under a stream of N_2, and dissolving the residue in basal buffer at a concentration of 1 μCi/μl. The final concentration of exogenous GABA was 3.6 μM, and the total amount of radioactivity transported was generally approximately 3×10^5 c.p.m. per sample. The loading proceeded for 12 min, and the reaction was stopped by adding 750 μl of basal buffer, and applying the suspension to a filtration sandwich composed of cellulose ester and glass fiber filters, as described previously (Turner et al., 1989, 1995a,b).

Measurement of GABA release from synaptosomes

Release was measured using a superfusion device in conjunction with a fraction collector modified from a phonograph turntable (Forbush, 1984; Turner et al., 1989). Synaptosomes were superfused with an appropriate stimulus buffer and fractions ranging from 15 ms (78 r.p.m.) to 100 ms (12 r.p.m.) were collected to measure release. Radioactivity in each fraction and the amount remaining on the filter at the end of the experiment were determined by adding 1.5 ml liquid scintillation cocktail (BioSafe II; Research Products Inc., Mt. Prospect, IL, USA) and counting in a Packard Tri-Carb 2100TR liquid scintillation analyzer.

The calcium channel blockers ω-conotoxin MVIIC and ω-conotoxin GVIA were prepared as 1.0 mM stock solutions in water, divided into 10 μl portions, and stored at −70 °C. Working stocks were prepared by diluting the concentrated solutions 10-fold with basal buffer that contained 1 mg/ml bovine serum albumin. These working solutions could be subjected to multiple freeze-thaw cycles without apparent loss of activity. ω-Conotoxin MVIIC and ω-conotoxin GVIA were purchased from Bachem (Torrence, CA, USA). All other reagents were purchased from Fluka.

Data analysis

All electrophysiological data were acquired with the "Pulse" acquisition program (HEKA Elektronik), stored on hard disk, and subsequently analyzed using the "MiniAnalysis" program from Jaejin Software (Decatur, GA, USA). For analysis of events, a given event was required to exceed a detection threshold set at the maximum of the noise level, which was 5 pA and an area under the curve (fc) threshold of 30 fc. The following characteristics of mIPSCs were determined: frequency, amplitude, rise time constant and decay time constant. Rise times were measured from 10 to 90% of the peak amplitude and events that exceeded 4 ms rise time were rejected. Spontaneous IPSCs and mIPSCs occurring during the entire recording time period were analyzed such that each sample contained hundreds of synaptic events. All electrophysiological data were incorporated in a data base (Excel, Microsoft Corporation) and statistical analyses of data performed by the SigmaStat software program (SPSS, Inc.). Statistical comparisons of the distribution of each of the IPSC parameters were performed with the Kolmogorov-Smirnov (K-S) two sample test, which tests the null hypothesis that two independent samples come from populations with identical location and dispersion (Goodman, 1954). Synaptosome data were analyzed using Microsoft Excel. Results were expressed as the ratio of c.p.m. in each fraction to the total radioactivity remaining on the filter (×100%). Data reported are the average of at least six separate experiments performed on different days with freshly prepared synaptosomes. Standard error values were generally less than 10%, and never exceeded 20%. In order to account for any time-dependent changes in release rates, the order of the experimental conditions was randomized for each experiment. All electrophysiological and synaptosome data were analyzed for statistical significance using the Student's *t*-test (two-tailed). Significance was defined at $P<0.05$. Data are given as the mean±standard error of the mean.

RESULTS

The electrophysiological results presented are based on stable whole-cell patch clamp recordings from 162 CA1 pyramidal cells. Of these cells, 10 were examined to determine the effects of 5-HT on spontaneous IPSCs (in control Ringers solution). All other cells were used in experiments designed to characterize the effects of 5-HT on mIPSCs (in Ringers solution containing TTx, CNQX and D-AP5). Only those cells that maintained stable conditions such as failure rate and access resistance were used for the analysis of IPSCs.

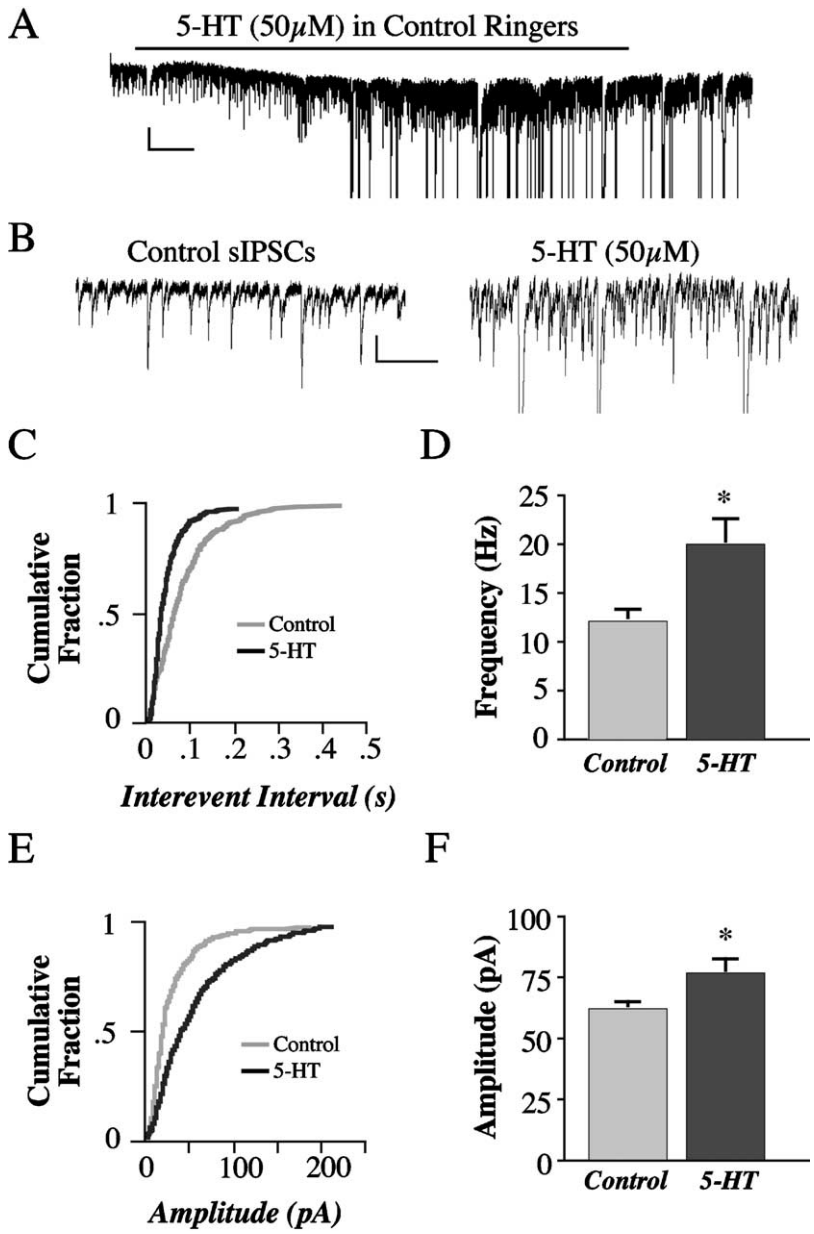

Fig. 1. 5-HT increases the frequency and amplitude of spontaneous IPSCs. (A) Representative current traces demonstrating the inward current and burst-like increase in the frequency and amplitude of spontaneous IPSCs in response to 5-HT (50 μM). Scale bar=100 pA, 5 s. (B) Representative current traces from the same cell shown in A, on an expanded time scale. Scale bar=100 pA, 500 ms. (C) Cumulative fraction plot of interevent intervals of spontaneous IPSCs in the presence of 5-HT compared with control in a representative cell ($P<0.0001$, K-S test). (D) Bar graph demonstrating the 5-HT induced increase in mean frequency of spontaneous IPSCs (* $P<0.001$). (E) Cumulative fraction plot of amplitudes of spontaneous IPSCs in the presence of 5-HT compared with control in a representative cell ($P<0.0001$, K-S test). (F) Bar graph demonstrating the 5-HT induced increase in mean amplitude of spontaneous IPSCs (* $P<0.01$).

5-HT increases the frequency and amplitude of spontaneous IPSCs

Bath application of 5-HT (10–100 μM) resulted in a small (41.2±3.2 pA) inward current, accompanied by a significant burst-like increase in the frequency of spontaneous IPSCs in eight of 10 CA1 pyramidal cells examined (from 12.1±1 Hz to 19.9±2.6 Hz; $P<0.001$; Fig. 1). Analysis of individual cells by the K-S test showed a significant shift in the distribution of spontaneous IPSCs to higher frequencies (shorter interevent intervals) in the presence of 5-HT ($P<0.01$–0.0001, Fig. 1C). The mean amplitude of spontaneous IPSCs also increased significantly, from baseline values of 61.6±3 pA under control conditions to 76.4±6 pA in the presence of 5-HT (Fig. 1F, $P<0.01$). Analysis of individual cells (Fig. 1E) showed a significant shift in the distribution of spontaneous IPSCs to higher amplitudes in the presence of 5-HT ($P<0.01$–0.0001, K-S test). The apparent increase in amplitude was likely due to the sum-

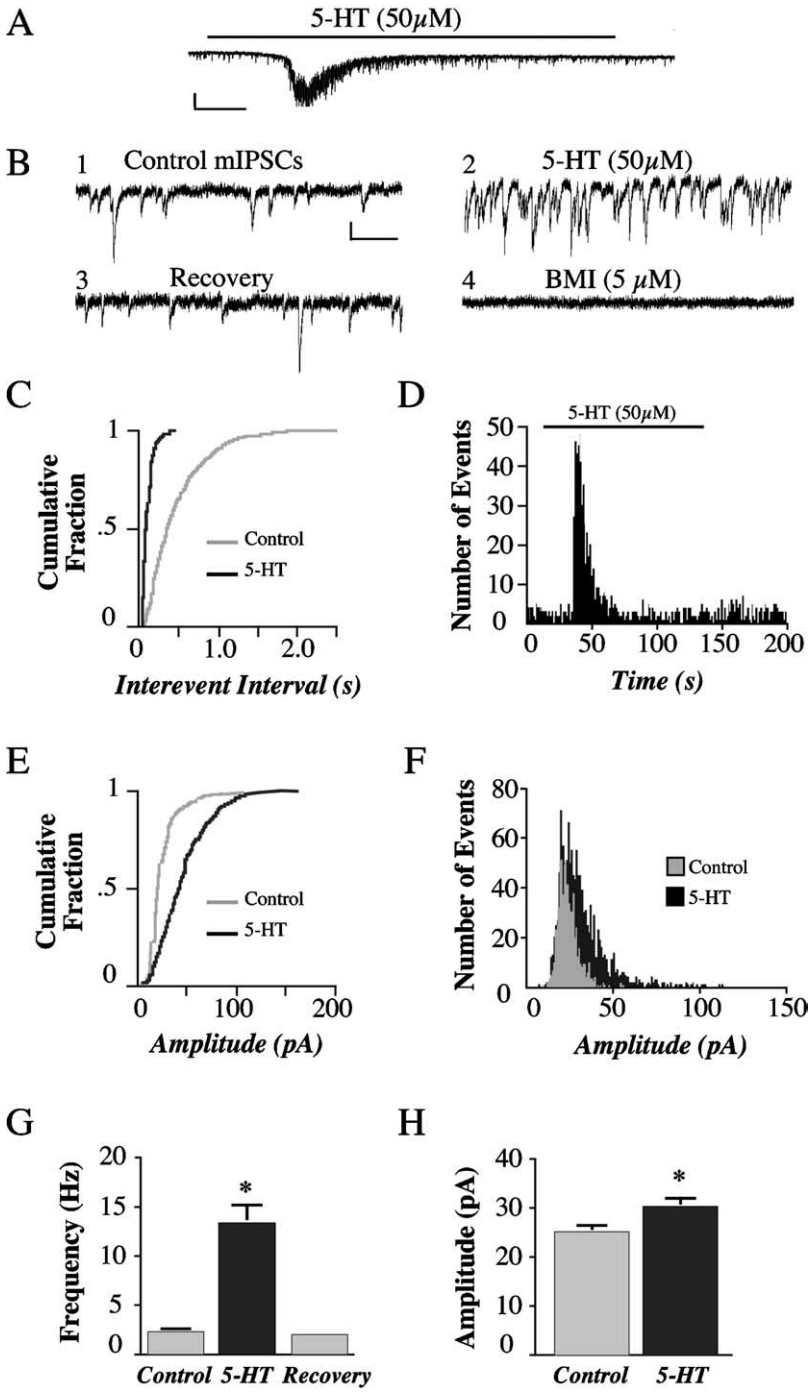

Fig. 2. Bath application of 5-HT increases the frequency and amplitude of $GABA_A$ receptor-mediated mIPSCs. (A) Representative current traces demonstrating the inward current and burst-like increase in mIPSC frequency and amplitude in response to 5-HT (50 μM). Scale bar=50 pA, 5 s. (B) Representative current traces from the same cell shown in A, on an expanded time scale. Traces show: control mIPSCs (1), mIPSCs in the presence of 5-HT (2), mIPSCs following recovery from 5-HT (3), and the complete block of the mIPSCs by bicuculline methiodide (4). Scale bar=20 pA, 500 ms. (C) Cumulative fraction plot demonstrating the significant decrease in interevent interval of mIPSCs in the presence of 5-HT compared with control in a representative cell ($P<0.0001$, K-S test). (D) Frequency-time histogram showing the effect of 5-HT on the number of mIPSCs over a 200 s recording period (1 s bins) in a representative cell. (E) Cumulative fraction plot demonstrating the significant shift to a greater number of high amplitude mIPSCs in the presence of 5-HT compared with control in a representative cell ($P<0.0001$, K-S test). (F) Frequency-amplitude histogram showing the effect of 5-HT on the frequency distribution of mIPSCs (1 pA bins) in a representative cell. (G) Bar graph demonstrating the significant increase in the mean frequency of mIPSCs elicited by 5-HT ($n=25$ cells, * $P<0.001$). (H) Bar graph demonstrating the significant increase in the mean amplitude of mIPSCs elicited by 5-HT ($n=25$ cells, * $P<0.05$).

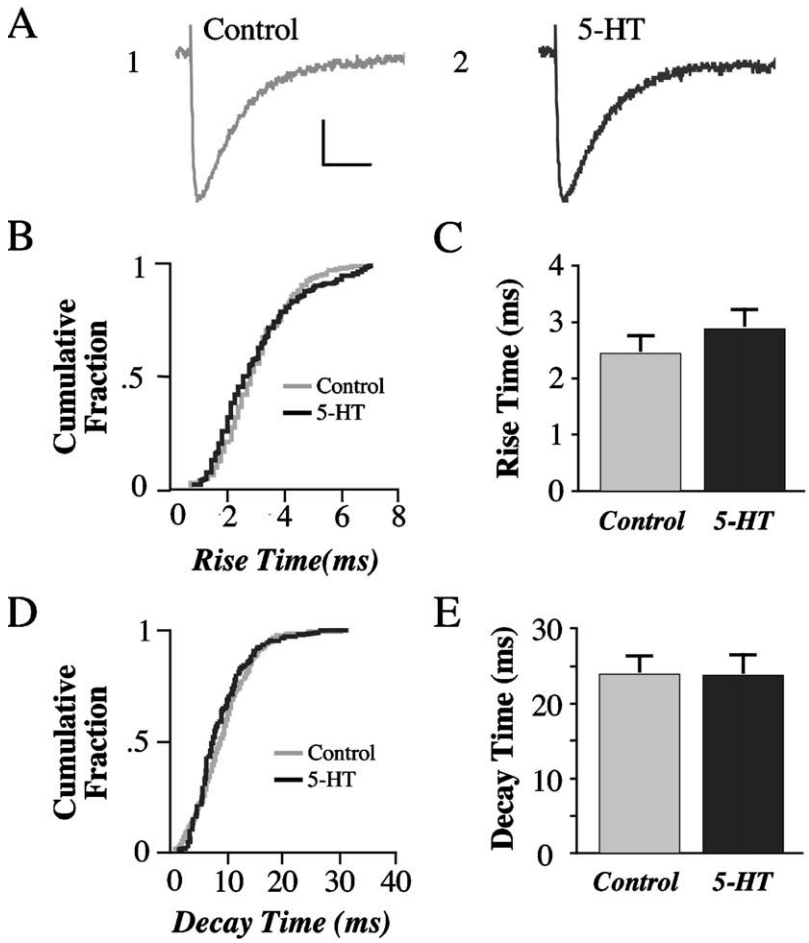

Fig. 3. 5-HT does not change mIPSC kinetics. (A) Grouped averages of events from a representative cell under control conditions (trace 1; average of 268 events) and in the presence of 5-HT (50 μM; trace 2; average of 488 events). Traces are normalized to control mIPSC amplitude. Scale bar=5 pA, 20 ms. (B) Cumulative fraction plot demonstrating no difference in the distribution of mIPSC rise times in the presence of 5-HT compared with control in a representative cell. (C) Bar graph demonstrating no significant effect of 5-HT on the mean rise time of mIPSCs (n=25 cells). (D) Cumulative fraction plot demonstrating no difference in the distribution of mIPSC decay times in the presence of 5-HT compared with control in a representative cell. (E) Bar graph demonstrating no significant effect of 5-HT on the mean decay time of mIPSCs (n=25 cells).

mation of lower amplitude events that occur at greatly increased frequency. This hypothesis is supported by the finding that the majority of the high amplitude events were composed of multiple events occurring almost simultaneously and thus summing.

5-HT increases the frequency and amplitude of $GABA_A$ receptor-mediated mIPSCs

$GABA_A$ receptor-mediated mIPSCs were recorded under conditions in which sodium-dependent action potentials and glutamatergic synaptic responses were fully blocked (TTx, 600 nM; CNQX, 10 μM; D-AP5, 40 μM). mIPSCs reversed at 0 mV, the equilibrium potential for Cl^- in these studies (not shown), and were completely abolished by the application of the specific $GABA_A$ receptor antagonist bicuculline methiodide (5 μM, 20/20 cells, Fig. 2B_4).

In 63% (25/40) of the cells tested, bath application of 5-HT (10–100 μM) resulted in a dramatic burst-like increase in the frequency and amplitude of mIPSCs (Fig. 2), accompanied by an inward current with a mean amplitude of 31±3.4 pA. In the other 37% (15/40) of the cells examined, 5-HT application produced no change in baseline mIPSC characteristics, but did induce an inward current with a mean amplitude of 36±3.7 pA (not shown). This 5-HT-induced postsynaptic inward current was blocked by application of propranolol HCl, which has been demonstrated to be an antagonist of the 5-HT_{1A} receptor (n=4/4, not shown). The mean frequency of mIPSCs increased over six-fold, from baseline control levels of 2.22±0.31 Hz to 13.3±1.75 Hz in the presence of 5-HT (P<0.001, Fig. 2A–D, G). Analysis of individual cells (Fig. 2C) showed a significant shift in the distribution of mIPSCs to decreased interevent intervals in the presence of 5-HT (P<0.01–0.0001, K-S test). The mean amplitude of mIPSCs was also slightly but significantly increased during the 5-HT-induced burst, from baseline values of 25±5 pA to 30±2.8 pA in the presence of 5-HT (P<0.05, Fig. 2E, F, H). Analysis of individual cells (Fig. 2E) showed a significant shift in the distribution of mIPSCs to higher amplitudes in the presence of 5-HT (P<0.05–0.001, K-S test). The burst-like

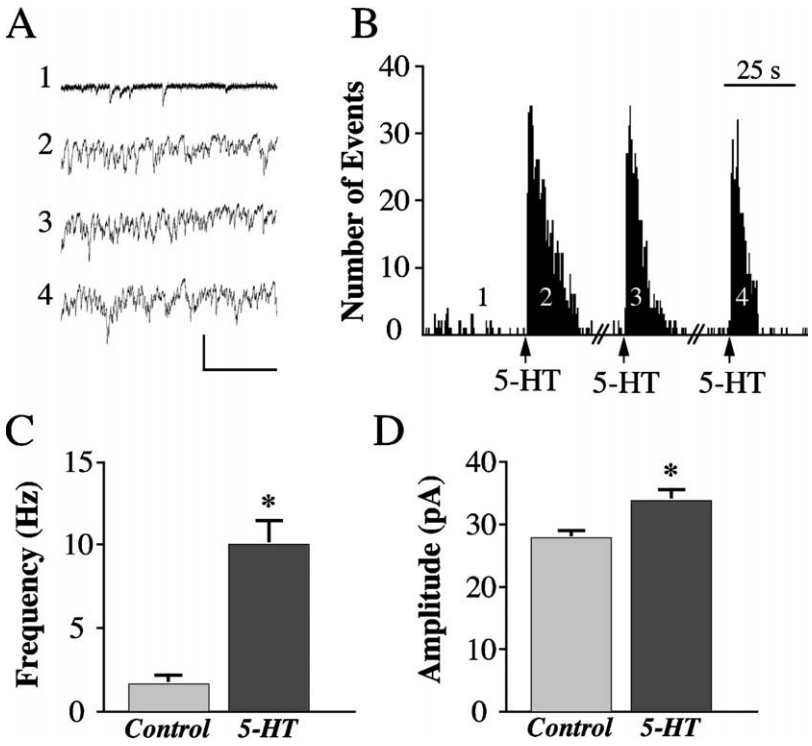

Fig. 4. Repetitive local applications of 5-HT increase the frequency and amplitude of mIPSCs. (A) Representative current traces demonstrating mIPSCs recorded under control conditions (trace 1) and in consecutive applications of 5-HT (traces 2–4). Traces were acquired at the time points indicated on the histogram in B. Scale bar=30 pA, 400 ms. (B) Frequency-time histogram showing the effects of three consecutive local applications of 5-HT on a representative cell. The diagonal cross-marks on the *x* axis indicate 5 min wash-out periods during which data were not acquired. (C) Bar graph demonstrating the significant increase in mIPSC frequency following local application of 5-HT (n=49 cells, * $P<0.001$). (D) Bar graph demonstrating the significant increase in mIPSC amplitude following local application of 5-HT (n=49 cells, * $P<0.05$).

increase in mIPSC frequency and amplitude in response to bath application of 5-HT decayed rapidly, returning to control values 15.3±2.6 s after the onset of the response (Fig. 2A, D). The apparent desensitization was irreversible under these recording conditions; following the initial bath application of 5-HT, no further response could be elicited by subsequent application of 5-HT, even following washout periods of ≥1 h (n=20 cells, not shown).

The kinetics of mIPSCs, determined by analyses of grouped averages of hundreds of events prior to and during 5-HT application, were unaltered by bath application of 5-HT (Fig. 3). The mean rise time of the events was well fit by a single exponential function and was 2.42±0.33 ms under control conditions compared with 2.87±0.33 ms in the presence of 5-HT (Fig. 3C). Similarly, the mean decay time constant, also well fit by a single exponential function, was unchanged at 23.9±2.4 ms under control conditions and 23.8±2.6 ms in the presence of 5-HT (Fig. 3E).

Local application of 5-HT increases the frequency and amplitude of mIPSCs

Local application of 5-HT (100 μM) via a pressure pipette elicited an inward current that was accompanied by a short-lasting burst-like increase in the frequency and amplitude of mIPSCs that was virtually identical to that seen with bath application of 5-HT (Fig. 4). Unlike with bath application however, multiple, consecutive responses could be elicited with the local application of 5-HT (Fig. 4A, B). In five cells examined to determine the number of 5-HT applications that could elicit a response, up to eight consecutive local applications of 5-HT (within 5 min intervals) were effective in eliciting a burst-like response of mIPSCs, with very little decrement in the magnitude of the response from application to application (Fig. 4). The repetitive application of 5-HT via pressure pipette allowed further pharmacological experiments, with measurements of 5-HT responses under control conditions, in the presence of altered extracellular media and recovery following washout of experimental media (see calcium and cadmium experiments described below).

Local application of 5-HT elicited a small (49.3±6 pA) inward current and a burst-like increase in the frequency and amplitude of mIPSCs that had a duration of 23±2.7 s. The rate of response desensitization was determined by fitting the frequency of events versus time with a single exponential function, yielding a decay time constant of 9.7±1.8 s. This burst-like facilitation of mIPSCs was observed in 70% (49/70) of the cells examined. The onset of the 5-HT induced burst was rapid, at between 0.1 and 1 s (presumably related to the distance of the drug delivery pipette and the recorded cell). 5-HT-induced a six-fold increase in mean frequency of mIPSCs with a control value of 1.63±0.53 Hz and a value of 10.03±1.4 Hz in the presence of 5-HT ($P<0.001$, Fig. 4C). The mean amplitude

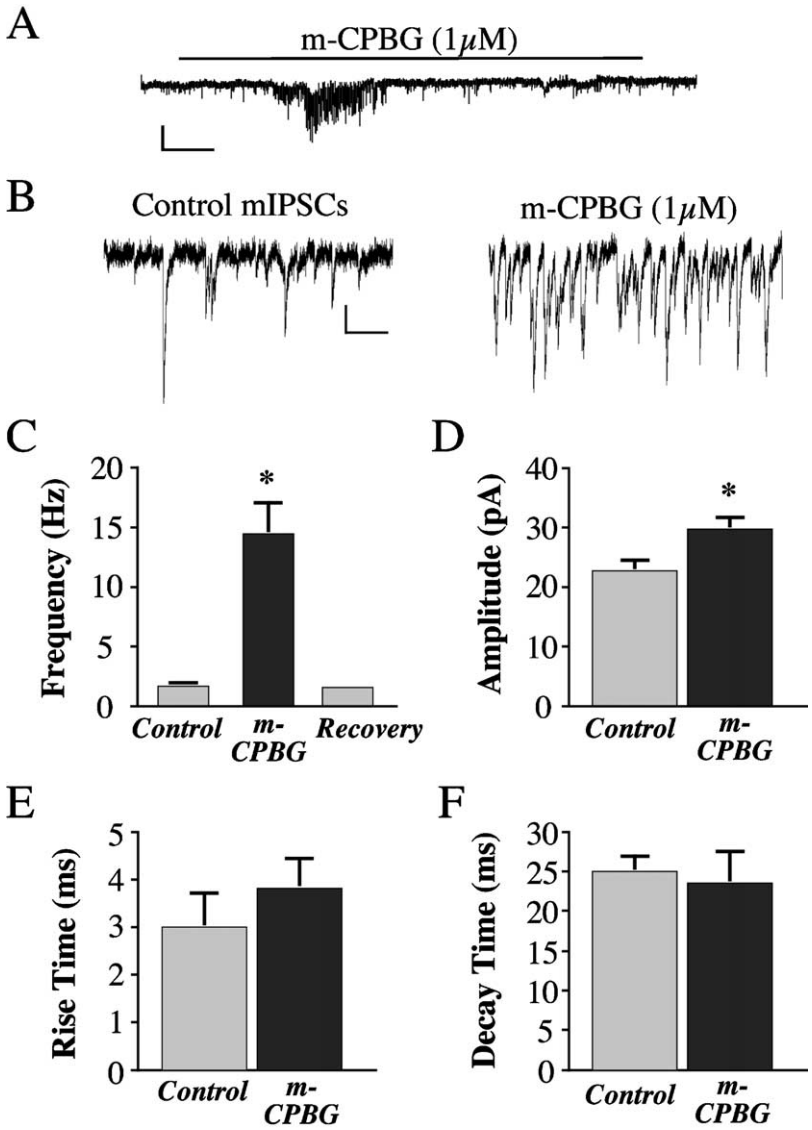

Fig. 5. 5-HT acts via 5-HT$_3$Rs to induce the transient increase in the frequency and amplitude of mIPSCs. (A) Representative current traces demonstrating the burst-like increase in mIPSCs in response to 1 μM *m*-CPBG. Scale bar=50 pA, 5 s. (B) Representative current traces from the same cell shown in A, on an expanded time scale. Scale bar=20 pA, 500 ms. (C, D) Bar graphs demonstrating the significant increases in the mean frequency (C; * $P<0.001$) and amplitude (D; * $P<0.05$) of mIPSCs elicited by *m*-CPBG ($n=11$ cells). (E, F) Bar graphs demonstrating no significant effect of *m*-CPBG on the mean rise time (E) or mean decay time (F) of mIPSCs ($n=11$ cells).

of mIPSCs was also significantly increased from 27.7±1.2 pA under control conditions to 33.8±1.8 in the presence of 5-HT ($P<0.05$, Fig. 4D).

The 5-HT induced increase in frequency and amplitude of mIPSCs is due to 5-HT$_3$R activation

The rapid onset, desensitization and facilitative nature of the 5-HT-mediated increase in frequency and amplitude of mIPSCs led to the investigation of whether this response was due to the activation of the 5-HT$_3$R as has been shown by others for 5-HT-mediated effects on *spontaneous* IPSPs (Ropert and Guy, 1991; Piguet and Galvan, 1994; Shen and Andrade, 1998). Bath or local application of the selective 5-HT$_3$R agonist *m*-CPBG (0.1–10 μM) closely mimicked the facilitative actions of 5-HT on mIPSCs in 65% (11/17) of the cells examined (Fig. 5). *m*-CPBG application did not result in an inward current in any of the cells examined. The mean frequency increased nine-fold, from 1.58±0.3 Hz (control) to 14.39±0.23 Hz (*m*-CPBG) and the mean amplitude also increased from 22.5±1.8 pA (control) to 29.5±2 pA (*m*-CPBG). The kinetics of events in the presence of *m*-CPBG were unaltered, with mean rise times of 3.0±0.7 ms (control) and 3.2±0.6 ms (*m*-CPBG) and mean decay times of 25.1±1.8 (control) and 23.4±4.1 ms (*m*-CPBG). The responses elicited by 5-HT and by *m*-CPBG were not statistically different, indicating that the 5-HT facilitation of mIPSCs is mediated via the activation of the 5HT$_3$R.

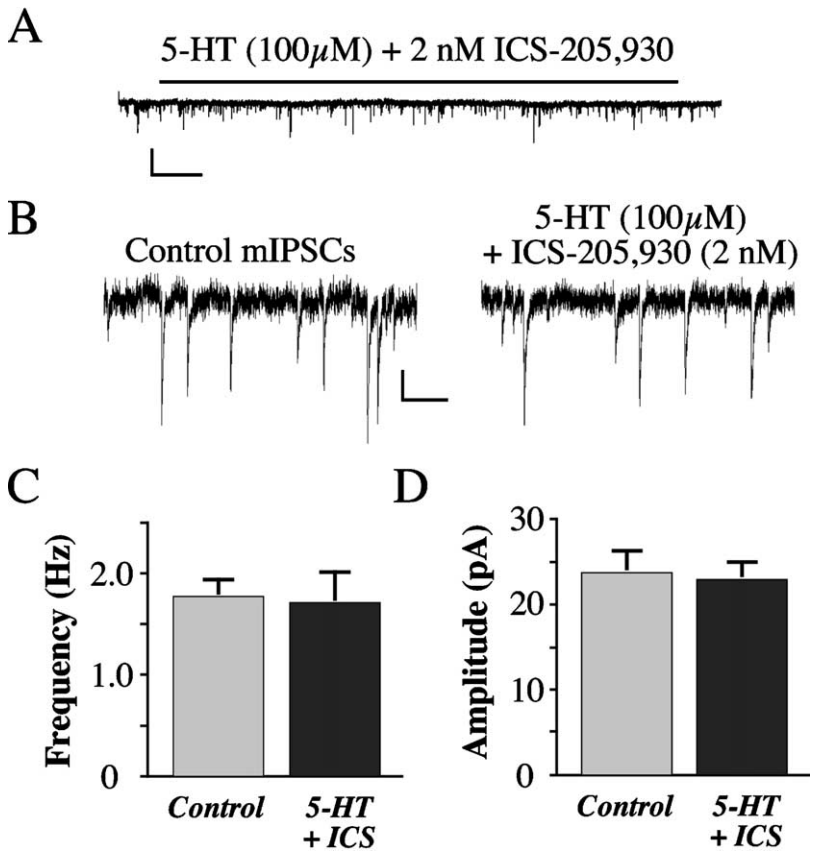

Fig. 6. Block of 5-HT-mediated facilitation of mIPSCs by the selective 5-HT_3R antagonist ICS-205,930. (A) Representative current traces demonstrating no effect of 5-HT in the presence of ICS-205,930 (2 nM). Scale bar=50 pA, 5 s. (B) Representative current traces from the same cell shown in A, on an expanded time scale. Scale bar=20 pA, 500 ms. (C, D) Bar graphs demonstrating no significant effect of 5-HT on the frequency (C) or amplitude (D) of mIPSCs in the presence of ICS-205,930 (n=25 cells).

The mediation of the 5-HT response by 5-HT_3Rs was confirmed by experiments in which 5-HT was bath applied in the presence of the specific 5-HT_3R antagonist ICS-205,930 (2 nM; Fig. 6). None of the cells examined responded to 5-HT with a burst of mIPSCs in the presence of this antagonist (25/25). Taken together, the *m*-CPBG and ICS-205,930 experiments confirm that the 5-HT-induced facilitation of mIPSC frequency and amplitude (and hence GABA release) is mediated by activation of 5HT_3Rs which are likely located on presynaptic nerve terminals of local inhibitory interneurons.

The 5-HT_3R-mediated transient increase in the frequency and amplitude of mIPSCs is Ca^{2+}-dependent

It was hypothesized that the 5HT_3R-mediated increase in mIPSC frequency and amplitude was likely a result of an increase in Ca^{2+} influx, either through activation of high voltage-activated (HVA) Ca^{2+} channels, directly through the 5HT_3R itself, or both. To test this hypothesis, comparisons of the response elicited by 5-HT in control Ringers solution (2.5 mM calcium), low calcium (15 μM) and finally in a 0 calcium solution (+2 mM EGTA) were made (Fig. 7). Local application of 5-HT in the presence of low (15 μM) calcium Ringers solution generated a burst-like increase in the frequency of mIPSCs from 2.9±0.4 Hz (control) to 13.4±2 Hz (5-HT) that was indistinguishable from the response seen in control Ringers solution (2.5 mM calcium) in all cells tested (n=15, Fig. 7A, B, F). The amplitude of mIPSCs was also significantly increased in the low calcium conditions, from a baseline mean of 25±2 pA (control) to 31.1±2.3 pA in the presence of 5-HT (not shown). In contrast, the application of 5-HT in the 0 calcium (+2 mM EGTA) solution fully and reversibly blocked the 5-HT-induced burst of mIPSCs in every cell examined (n=20, Fig. 7C–F). In addition, the response elicited by 5-HT in control Ringers solution (2.5 mM Ca^{2+}) was compared with that elicited in the presence of 100 μM cadmium, which blocks HVA Ca^{2+} channels (Fig. 8). The addition of 100 μM cadmium to the external solution fully and reversibly blocked the 5HT-induced burst of mIPSCs in every cell tested (n=10, Fig. 8A, B), providing further confirmation of the Ca^{2+}-dependence of the response.

The 5-HT receptor-elicited increase in GABA release is mediated by Ca^{2+} influx through the 5-HT_3R ionophore complex

Having demonstrated the Ca^{2+}-dependence of the facilitation of mIPSCs by 5-HT, experiments were performed to determine whether 5-HT_3R activation increases Ca^{2+} influx

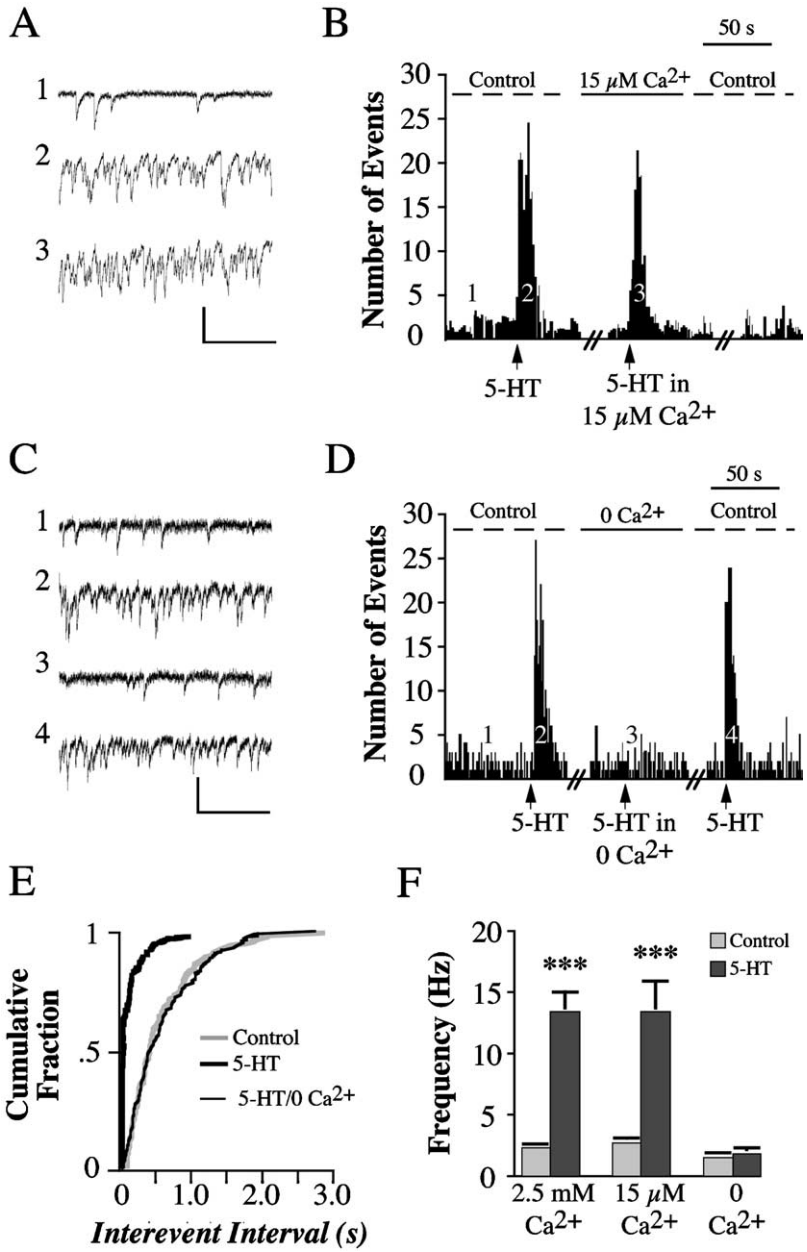

Fig. 7. The 5-HT_3R-mediated increase in the frequency and amplitude of mIPSCs is calcium-dependent. (A) Representative current traces demonstrating mIPSCs recorded under control conditions (trace 1), in the presence of 5-HT in control Ringers solution (trace 2) and in the presence of 5-HT in 15 μM extracellular calcium (trace 3). Traces were acquired at the time points indicated on the histogram in B. (B) Frequency-time histogram showing the effects of pressure pipette applications of 5-HT on a representative cell in control Ringers solution and in 15 μM extracellular calcium. The diagonal cross-marks on the *x* axis indicate a 5 min perfusion period during which data were not acquired. (C) Representative current traces demonstrating mIPSCs recorded under control conditions (trace 1), in the presence of 5-HT in control Ringers solution (trace 2), in the presence of 5-HT in 0 extracellular calcium (trace 3), and, following washout of the 0 calcium solution, in control Ringers solution (trace 4). Traces were acquired at the time points indicated on the histogram in D. (D) Frequency-time histogram showing the effects of pressure pipette applications of 5-HT on a representative cell in control Ringers solution, in 0 calcium solution and following washout of the 0 calcium solution, in control Ringers solution. The diagonal cross-marks on the *x* axis indicate a 15 min perfusion period during which data were not acquired. (E) Cumulative fraction plot demonstrating the significant decrease in interevent interval of mIPSCs in the presence of 5-HT (thick black line) compared with control (gray line) and to 5-HT in 0 calcium solution (thin black line) in a representative cell ($P<0.0001$, K-S test). (F) Bar graph demonstrating the significant increase in the mean frequency of mIPSCs elicited by 5-HT in control Ringers solution (2.5 mM calcium ($n=26$ cells, $P<0.001$, Student's *t*-test), in low calcium Ringers solution (15 μM calcium ($n=15$ cells, $P<0.001$, Student's *t*-test), and in 0 calcium solution ($n=20$ cells, not significant). Scale bars=30 pA in A and C, 400 ms.

indirectly by activating HVA Ca^{2+} channels located on the presynaptic terminal, or *directly* due to Ca^{2+} influx through the 5-HT_3R-ionophore complex itself. Ronde and Nichols (1998) and Nayak et al. (1999) have shown that the 5-HT_3R is highly permeable to Ca^{2+} and that Ca^{2+} influx through these channels can be discriminated from influx through HVA Ca^{2+}

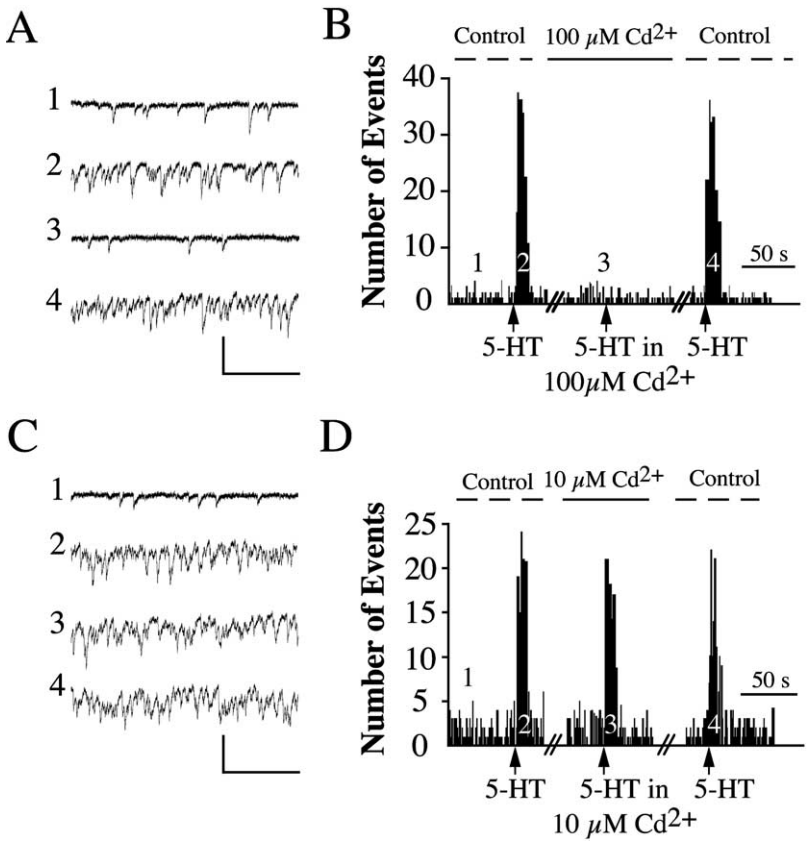

Fig. 8. The 5-HT_3R-elicited increase in GABA release is mediated, in part, by calcium influx through the 5-HT_3R ionophore complex itself. (A) Representative current traces demonstrating mIPSCs recorded under control conditions (trace 1), in the presence of 5-HT in control Ringers solution (trace 2), in the presence of 5-HT in 100 μM cadmium (trace 3), and, following washout of the 100 μM cadmium, in control Ringers solution (trace 4). Traces were acquired at the time points indicated on the histogram in B. Scale bar=30 pA, 400 ms. (B) Frequency-time histogram showing the effects of pressure pipette applications of 5-HT on a representative cell in control Ringers solution, in 100 μM cadmium and following washout of the 100 μM cadmium solution, in control Ringers solution. The diagonal cross-marks on the *x* axis indicate 20 min wash-out periods during which data were not acquired. (C) Representative current traces demonstrating mIPSCs recorded under control conditions (trace 1), in the presence of 5-HT in control Ringers solution (trace 2), in the presence of 5-HT in 10 μM cadmium (trace 3), and, following washout of the 10 μM cadmium, in control Ringers solution (trace 4). Traces were acquired at the time points indicated on the histogram in D. Scale bar=30 pA, 400 ms. (D) Frequency-time histogram showing the effects of pressure pipette applications of 5-HT on a representative cell in control Ringers solution, in 10 μM cadmium and following washout of the 10 μM cadmium solution, in control Ringers solution. The diagonal cross-marks on the *x* axis indicate 20 min wash-out periods during which data were not acquired.

channels based on differential sensitivity of the two classes of channels to the divalent cation cadmium. Ten micromolar cadmium is sufficient to block Ca^{2+} influx through HVA Ca^{2+} channels but *not* Ca^{2+} influx through the 5-HT_3R, while 100 μM cadmium blocks Ca^{2+} influx through both HVA Ca^{2+} channels and through the 5-HT_3R (Ronde and Nichols, 1998). As noted, the application of 100 μM cadmium fully and reversibly blocked the 5HT-induced burst of mIPSCs (Fig. 8A, B). In contrast, the burst-like response of mIPSCs to 5-HT application was preserved in the presence of 10 μM cadmium (n=10, Fig. 8C, D). These data strongly support the hypothesis that Ca^{2+} influx through the 5-HT_3R-ionophore complex itself plays an important role in the facilitation of GABA release.

5HT alters synaptic vesicle dynamics in hippocampal synaptosomes

Electrophysiological data strongly support the hypothesis that the 5-HT-induced increase in the release of GABA is due, in large part, to increased Ca^{2+} influx through presynaptic 5HT_3Rs. In an effort to study the biochemical basis of this effect, we utilized hippocampal synaptosomes where pharmacological equilibrium is unequivocal and presynaptic mechanisms can be studied in isolation. We first examined whether we could replicate the action of 5-HT on electrophysiological measures of GABA release (i.e. increased mIPSC frequency) by continuous application of 5-HT (100 μM) or *m*-CPBG (10 μM) to hippocampal synaptosomes labeled with [^{3}H]GABA to determine whether [^{3}H]GABA release rates were altered. Contrary to expectations, we did not observe a significant increase in the rate of radiolabel efflux in response to agonist applications lasting up to 10 s (data not shown). We suspect that this was due to the relatively small contribution of 5HT_3R-mediated exocytosis when compared with basal GABA release from all possible sources in synaptosomes. In particular, [^{3}H]GABA efflux from the cytoplasm mediated by reversal of the Na^+-dependent, nipecotic acid sensitive

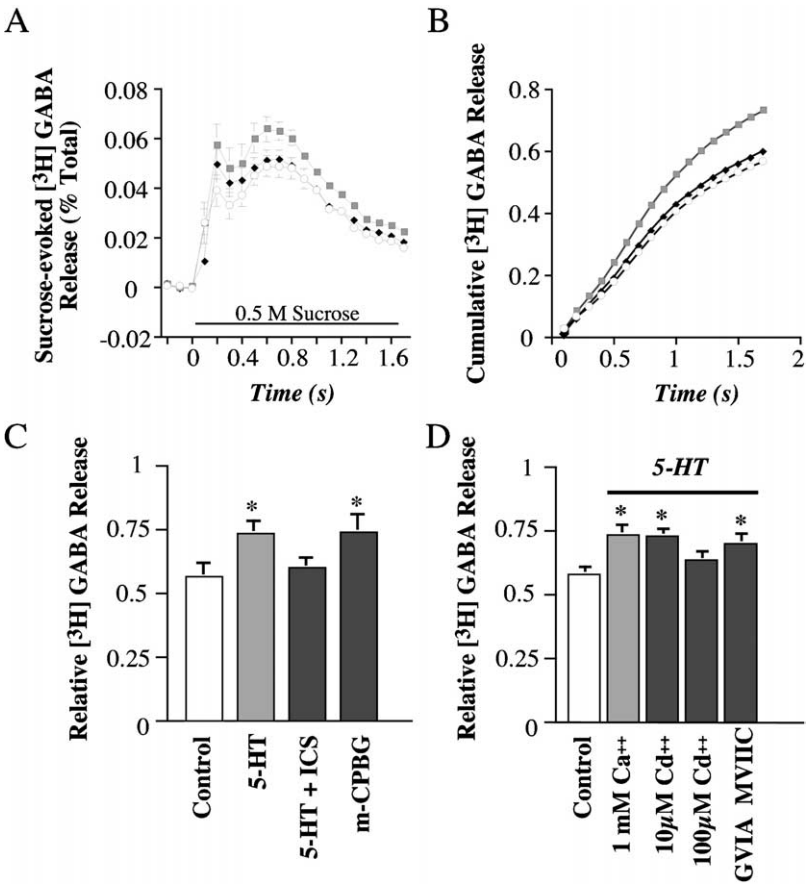

Fig. 9. The 5-HT-induced increase in osmotically evoked [^{3}H]GABA release is mediated by Ca^{2+} influx via the $5HT_3R$. (A) Synaptosomes were stimulated using saline alone (○), 100 μM 5-HT (▨), or 100 μM 5-HT plus 1 μM ICS-205,930 (♦). The ability of hypertonic saline to evoke [^{3}H]GABA release was enhanced by 5-HT, and the enhancement was blocked by the 5-HT selective receptor antagonist ICS-205,930. Error bars indicate the S.E.M. (B) Cumulative plot of sucrose-evoked [^{3}H]GABA release. (C) Pharmacological identification of the 5-HT receptor that mediates the enhancement. 5-HT-enhanced release (* $P<0.01$) was blocked by the 5-HT-selective antagonist ICS-205,930 (ICS), and was simulated by the $5HT_3R$ agonist *m*-CPBG (10 μM, * $P<0.04$). (D) The Ca^{2+} dependence is mediated by the $5HT_3R$, since 100 μM (but not 10 μM) Cd^{2+} blocks the effects and ω-conotoxin GVIA and ω-conotoxin MVIIC, specific antagonists of N- and P/Q-type neuronal Ca^{2+} channels, were without effect on 5-HT enhanced release. * $P<0.02$. Data are expressed as the mean of 36–38 individual determinations (±S.E.M.).

transporter may represent a large background signal that masked a relatively small 5-HT evoked [^{3}H]GABA release.

Relatively small increases in cytoplasmic Ca^{2+} concentrations have been shown to alter the distribution of synaptic vesicles between a reserve pool and one or more releasable pools (RP; Rosenmund and Stevens, 1996; Smith et al., 1998; Stevens and Wesseling, 1998; Sakaba and Neher, 2001). We used hypertonic saline solutions to evoke exocytosis without changes in intracellular Ca^{2+} concentrations in order to assess whether activation of presynaptic $5HT_3Rs$ altered the size or refilling of the RP of GABA in hippocampal synaptosomes. We first applied five, 200 ms conditioning pulses of saline that contained either 100 μM 5-HT or control saline at 10 s intervals, to minimize the amount of $5HT_3R$ desensitization. One second after the fifth conditioning pulse, we applied a hypertonic saline solution that contained 0.5 M sucrose to evoke an osmotic pressure-induced, Ca^{2+}-independent exocytotic event.

Control synaptosomes that had been conditioned using only saline (no 5-HT) were exposed to saline containing 0.5 M sucrose to induce osmotically evoked [^{3}H]GABA release. The release event was relatively slow when compared with depolarization-evoked exocytosis (Turner and Dunlap, 1995a,b); release rates increased to a maximum within 0.4–0.6 s and subsequently decayed over 1–2 s to a plateau rate that remained elevated above basal release rates measured using normal, isotonic saline (Fig. 9A). Synaptosomes that had been conditioned using saline that contained 100 μM 5-HT showed a significant, 27±10.2% increase in the amount of osmotically evoked exocytosis ($P<0.03$).

The kinetics of osmotically evoked [^{3}H]GABA exocytosis were analyzed by calculating the cumulative release as a function of time, then using a non-linear least squares method to fit the data with the sum of an exponential component plus a linear component (Fig. 9B). By analogy to previous studies on osmotically evoked neurosecretion, these kinetic components presumably represent the rapid exocytosis of the RP of synaptic vesicles summated with the linear release of vesicles recruited into the RP from a reserve pool upon the depletion of the RP (Stevens and Sullivan,

1998). The exponential component of release from synaptosomes that had been stimulated by 5-HT was not significantly different than control (0.629±0.059% [n=23]), but both the slope of the linear component (0.114±0.003%-s^{-1}, P<0.05) and the cumulative integral observed at the end of a 3.3 s pulse were significantly increased relative to control (1.103±0.055% vs. 0.870±0.034%, P<0.02). As integration of release tends to improve the signal-to-noise ratio for these measurements, we used the integrated release after a 1.6-s pulse (the time required for 95% decay of the exponential component) for subsequent evaluation of the 5-HT response in hippocampal synaptosomes.

The pharmacology of the 5-HT-induced increase in the size of the RP was explored by using 5-HT receptor selective ligands (Fig. 9). When the five-pulse protocol was delivered with 10 μM ICS-205,930, a selective $5HT_3R$ antagonist, in the stimulus buffer, the ability of 100 μM 5-HT to enhance osmotically evoked [^{3}H]GABA release was largely eliminated (Fig. 9A). When the release integral was calculated (Fig. 9B), it was found that 5-HT treatment resulted in a significant increase in osmotically evoked release when compared with untreated synaptosomes (0.732±0.053% vs. 0.565±0.052%, P<0.01 [n=5]). Further, the $5HT_3R$ agonist *m*-CPBG was nearly as effective as 5HT in enhancing osmotically evoked release of [^{3}H]GABA (0.739±0.071% vs. 0.565±0.052%, P<0.04 [n=11]). Both observations indicate that the $5HT_3R$ subtype mediates the ability of 5-HT to enhance the osmotically evoked [^{3}H]GABA release in terminals as observed in the electrophysiological studies.

Like other members of the ligand-gated channel superfamily, the $5HT_3R$ is a non-selective cation channel that is highly permeant to Ca^{2+}. Thus, activating the receptor could mediate Ca^{2+} influx directly, or the resulting depolarization could indirectly trigger Ca^{2+} entry by activating voltage-gated calcium channels. We performed a set of experiments designed to evaluate these possibilities by selectively blocking voltage-gated Ca^{2+} channels and by blocking the Ca^{2+} permeability of 5-HT-gated channels (Fig. 9D). We first compared the effect of 10 and 100 μM Cd^{2+}, since 10 μM Cd^{2+} will preferentially block voltage-gated Ca^{2+} channels, whereas 100 μM will block the $5HT_3R$ as well. In the presence of 10 μM Cd^{2+}, 5-HT enhanced [^{3}H]GABA release to the same extent as 5-HT alone (0.727±0.032% vs. 0.732±0.042% [n=18], control vs. 5-HT+10 μM Cd^{2+}, P<0.02). In contrast, 100 μM Cd^{2+} nearly eliminated the 5-HT enhancement (0.632±0.035 vs. 0.580±0.029 [n=18]; control vs. 5-HT+100 μM Cd^{2+}, P>0.05). When synaptosomes were pretreated with ω-conotoxin GVIA plus ω-conotoxin MVIIC (1 μM each), saturating concentrations of peptide antagonists selective for N- and P/Q-type neuronal Ca^{2+} channels (Turner and Dunlap, 1995a), 5-HT also enhanced the RP over control (0.699±0.038% vs. 0.580±0.029%; control vs. 5-HT+GVIA/MVIIC, P<0.02 [n=11]). Taken together, these results support the hypothesis that synaptic vesicle dynamics are altered by Ca^{2+} entry into synaptosomes directly through the $5HT_3R$ ionophore.

DISCUSSION

Using both electrophysiological and biochemical measures of GABA release, we have demonstrated that: 1) serotonin acts presynaptically to increase the release of GABA; 2) serotonergic facilitation of GABA release is mediated by the $5HT_3R$ subtype; 3) the increase in GABA release is Ca^{2+}-dependent; and 4) the facilitation of GABA release is primarily due to Ca^{2+} influx directly through the $5HT_3R$.

Serotonin acts at presynaptic receptors to facilitate GABA release

In agreement with earlier reports using *in vitro* slices (Ropert and Guy, 1991; Shen and Andrade, 1998) the present study demonstrated a 5-HT-induced increase in the frequency and amplitude of spontaneous IPSCs in CA1 pyramidal cells. The presumed block of the 5-HT-elicited facilitation of IPSCs by the sodium channel blocker TTx in previous slice studies led to the hypothesis that 5-HT increases GABA release not directly by presynaptic mechanisms, but rather indirectly through excitation (via $5HT_3Rs$) of interneurons. This is consistent with the finding that hippocampal interneurons are depolarized by $5\text{-}HT_3R$ agonists (Kawa, 1994; McMahon and Kauer, 1997). However, in contrast to these earlier reports (and in agreement with a recent study by Katsurabayashi et al., 2003, using mechanically dissociated CA1 pyramidal cells) we demonstrate that the facilitation of GABA release by 5-HT persists in the presence of TTx in a majority of CA1 pyramidal cells examined in *in vitro* slices. This finding, together with our independent measurement of 5-HT-induced GABA release from synaptosomes, provides further persuasive evidence that 5-HT acts presynaptically to facilitate GABA release.

We observed that hippocampal CA1 pyramidal cells are heterogeneous in terms of their response to 5-HT and to *m*-CPBG. It is likely that different populations of CA1 pyramidal cells receive direct synaptic inputs from different classes of inhibitory interneurons, some of which possess presynaptic $5HT_3Rs$ and others of which do not. Indeed only about 50% of hippocampal interneurons express $5HT_3Rs$ (Miettinen and Freund, 1992a,b; Acsády et al., 1993; Papp et al., 1999; Morales and Bloom, 1997). For example, both calbindin-containing interneurons in the stratum radiatum and CCK/VIP binding basket cells express $5HT_3Rs$ while another basket cell population, the parvalbumin positive perisomatic inhibitory cells, do not express $5HT_3Rs$ (Morales and Bloom, 1997). Thus the unresponsive CA1 pyramidal cells, while clearly receiving significant GABAergic input (as evidenced by their high baseline frequency of spontaneous and mIPSCs) are likely not innervated by interneurons that possess $5HT_3Rs$.

Given the heterogeneity of CA1 pyramidal cell responses to 5-HT application, it is possible that differences in the numbers of cells sampled in the present compared with previous studies account for the different results. While two thirds of the 152 cells examined in this study responded to 5-HT or to the selective $5\text{-}HT_3R$ agonist *m*-CPBG with a dramatically increased frequency and amplitude of mIPSCs, one third of the cells examined dis-

played no alteration in mIPSC characteristics. This heterogeneity of CA1 pyramidal cells in terms of response to 5-HT_3R activation emphasizes the necessity of sampling sufficient numbers of cells in these studies.

The 5-HT-induced increase in GABA release is 5-HT_3R mediated

The 5-HT-mediated increase in frequency and amplitude of mIPSCs was characterized by a rapid onset and significant degree of desensitization; these response characteristics were similar to those reported earlier by other investigators who demonstrated that the 5-HT-mediated increase in frequency of spontaneous (Ropert and Guy, 1991; Piguet and Galvan, 1994; Shen and Andrade, 1998) or, in other systems, mIPSPs (Koyama et al., 2000, 2002; Katsurabayashi et al., 2003) was due to the activation of 5-HT_3 serotonin receptors. We observed that the 5-HT-mediated facilitation of mIPSC frequency and amplitude, and the osmotically evoked GABA release from synaptosomes, was mimicked by the selective 5-HT_3R agonist *m*-CPBG and blocked by the selective 5-HT_3R antagonist ICS-205,930, confirming the role of the 5-HT_3R in the facilitation of GABA release. These results extend the findings of Katsurabayashi and co-workers (2003) regarding the functional role of presynaptic 5-HT_3Rs in the hippocampus. Given the presence of both 5-HT_{1A}Rs and 5-HT_3Rs on presynaptic boutons in the hippocampus, (Katsurabayashi et al., 2003) and a previously reported 5-HT_{1A}R-mediated inhibition of GABA release (Schmitz et al., 1995; Koyama et al., 1999, 2002; Katsurabayashi et al., 2003), an ICS-205,930-resistant component to 5-HT mediation of GABA release was expected in the present studies. However, following application of ICS-205,930, no further response to 5-HT was seen in these experiments; thus there was no evidence for a role of other serotonin receptor subtypes, including 5-HT_{1A}Rs, in the modulation of GABA release.

GABA release is facilitated by direct Ca^{2+} influx through the 5-HT_3R

Given previous findings in mechanically dissociated basolateral amygdala neurons (Koyama et al., 2000), our working hypothesis was that a similar mechanism for a 5HT_3R-mediated increase in GABA release exists in the hippocampal slice, namely, that GABA release is facilitated due to increases in presynaptic Ca^{2+} mediated by Ca^{2+} influx through the 5HT_3R ionophore. The 5-HT-mediated increase in GABA release was fully and reversibly blocked by application of 5-HT in 0 Ca^{2+} and in 100 μM cadmium-containing solutions in both mIPSC and synaptosome studies, providing direct evidence for the Ca^{2+}-dependence of the response. It is known from neurochemical studies that 5HT_3Rs are located on presynaptic nerve terminals in the CA1 pyramidal cell layer and that these receptors are highly permeable to Ca^{2+}, unlike the 5HT_3Rs located on neuronal somata, which appear to be largely permeable to sodium and potassium (Nichols and Mollard, 1996; Ronde and Nichols, 1998; Nayak et al., 1999). Ca^{2+} influx through the 5HT_3R was blocked by high (100 μM) but not by low (10 μM) concentrations of cadmium, whereas HVA Ca^{2+} channels located on presynaptic terminals are largely blocked by 10 μM cadmium (Ronde and Nichols, 1998). Likewise, the 5HT_3R-mediated increase in GABA release, as reflected by increases in mIPSC frequency, was unaffected by 10 μM Cd^{2+}, but blocked by 100 μM Cd^{2+}, suggesting that Ca^{2+}influx directly through the 5HT_3R, rather than through activation of HVA Ca^{2+} channels, plays a primary role in facilitating GABA release. Direct measures of GABA release from synaptosomes support this hypothesis, since the 5-HT-induced increase in response to hypertonic saline was largely resistant to 10 μM cadmium or to peptide inhibitors of HVA Ca^{2+} channels. These findings are consistent with those previously reported for mechanically dissociated basolateral amygdala neurons (Koyama et al., 2000).

Ca^{2+} entry and facilitation of GABA release

Perhaps the most significant questions left unanswered by our study are first, how does Ca^{2+} entry through the 5HT_3R facilitate GABA release? and second, how is this facilitated release related to changes in synaptic vesicle dynamics and mIPSC frequency? As for the first question, the simplest hypothesis is that Ca^{2+} entering through the 5HT_3R interacts with the active zone Ca^{2+} sensor, promoting synaptic vesicle fusion and exocytosis. However, available evidence argues against such a hypothesis. The Ca^{2+} sensitivity of the exocytosis process is thought to be relatively low, such that Ca^{2+} concentrations in excess of 10 μM are required to elicit vesicle fusion (Fernandez-Chacon et al., 2001). Further, it is believed that HVA Ca^{2+} channels are structurally integrated into the exocytotic machinery to enhance the probability of release by bringing the Ca^{2+} source into close proximity with the sensor. It seems unlikely (or at least unproven) that such a proximal structural relationship exists for presynaptic 5HT_3Rs. Finally, we observed 5-HT-induced facilitation of GABA release at extracellular Ca^{2+} concentrations as low as 15 μM, making it highly unlikely that the same low affinity Ca^{2+} sensor thought to regulate exocytosis is responsible for 5-HT-induced increases in the frequency of mIPSCs. Rather, it is more likely that a high-affinity calcium sensor is responsible for coupling 5HT_3R activation to the increase in mIPSC frequency seen in our study.

The second unresolved question revolves around 5-HT induced changes in synaptic vesicle dynamics and the relationship between these dynamics and miniature exocytotic events. We were surprised that we did not observe significant 5-HT-evoked release of [^{3}H]GABA in the synaptosomal preparation that could serve as a biochemical correlate of the electrophysiological findings in slices. The technical difficulties associated with measuring a potentially small change in isotope efflux from a temporally discrete burst of miniature release events is the most likely explanation for the failure to observe evoked release. It cannot be ruled out, however, that the difference in the 5-HT effect on the release of GABA in synaptosomes versus slices is due to species (mice vs. rat) and/or age

(juvenile vs. adult) differences. However, we did observe a significant 5-HT-induced increase in the synaptosomal response (GABA release) to hyperosmotic stimulation used to measure the RP of synaptic vesicles. How Ca^{2+} entry via the $5HT_3R$ leads to the observed response is unknown, but there is considerable evidence that Ca^{2+} can alter the synaptic vesicle refilling rates upon depletion (Rosenmund and Stevens, 1996; Smith et al., 1998; Stevens and Wesseling, 1998; Sakaba and Neher, 2001). Thus, the most reasonable explanation of the action of 5-HT on synaptic vesicle dynamics in response to hyperosmotic stimulus is that $5HT_3R$-mediated Ca^{2+} entry accelerates refilling of the active zones upon depletion. That is, when the osmotic pressure promotes the exocytosis of vesicles in the active zone, the rate of active zone refilling with new vesicles is enhanced due to the elevated Ca^{2+} concentration that results from presynaptic $5HT_3R$ activity. This mechanism has been demonstrated for α-7 nicotinic receptor-mediated regulation of dopamine release in striatum (Turner, 2004).

To conclude, we have measured 5-HT-mediated effects on GABA release in two separate preparations, in each of which the 5-HT effects appear to be related to presynaptic GABA release and storage. In both preparations, 5-HT induced increases in GABA release were mediated by a presynaptic $5HT_3R$ and were clearly Ca^{2+}-dependent. These findings are in agreement with previous findings in mechanically dissociated basolateral amygdala neurons (Koyama et al., 2000) and extend the observations of Katsurabayashi et al. (2003) regarding the mechanism of facilitation of GABA release by presynaptic $5HT_3Rs$ in the hippocampus. A central mechanistic question is whether changes in synaptic vesicle dynamics cause a transient increase in vesicle exocytosis. This question remains the focus of ongoing experiments.

Functional implications of presynaptic $5HT_3R$ activity

There has been increasing interest in the therapeutic potential of agents acting at the $5HT_3R$ in neuropsychiatric disorders (for review: Bentley and Barnes, 1995; Marek and Aghajanian, 1998). While their clinical relevance is still controversial, numerous *in vivo* studies utilizing 5-HT_3 agonists and antagonists have revealed an important role for this receptor in behavioral function; these pharmacological studies have revealed that the $5HT_3R$ plays a role in the modulation of anxiety, cognition, psychosis and addictive behavior (Costall et al., 1990, 1993; Nevins and Anthony, 1994; for review: Barnes and Sharp, 1999). Clearly, the activation of the $5HT_3R$ results in a significant, pulsatile increase in inhibition in the CA1 subfield that is temporally discrete but high in magnitude. This increase in inhibitory tone produced by serotonin may underlie, in part, the therapeutic responses recently observed in response to pharmacologic agents that act at the $5HT_3R$.

Acknowledgments—Supported by NIH grant HD22539 to J.I.L. and D.J.M., and NSF grant IBN-0218619 to T.J.T. We thank Dr. Kathleen Dunlap for helpful discussions and careful reading of this manuscript, Dr. Simon Levy for Ca^{2+} concentration measurements, and Susan O'Brien and Lisa Mangiamele for excellent technical assistance.

REFERENCES

Acsády L, Halasy K, Freund TF (1993) Calretenin is present in non-pyramidal cells of the rat hippocampus: III. Their inputs from the median raphe and medial septal nuclei. Neuroscience 52:829–841.

Andrade R (1998) Regulation of membrane excitability in the central nervous system by serotonin receptor subtypes. Ann NY Acad Sci 861:190–203.

Barnes NM, Sharp T (1999) A review of central 5-HT receptors and their function. Neuropharmacology 38:1083–1152.

Bentley KR, Barnes NM (1995) Therapeutic potential of 5-HT_3 receptor antagonists in neuropsychiatric disorders. CNS Drugs 3:363–392.

Blandina P, Goldfarb J, Craddock-Royal B, Green JP (1989) Release of endogenous dopamine by stimulation of 5-hydroxytryptamine$_3$ receptors in rat striatum. J Pharmacol Exp Ther 251:803–809.

Chen J, van Praag HM, Gardner EL (1991) Activation of 5-HT_3 receptor by 1-1-phenylbiguanide increases dopamine release in the rat nucleus accumbens. Brain Res 543:354–357.

Costall B, Naylor RJ, Tyers MB (1990) The psychopharmacology of 5-HT_3 receptors. J Pharmacol Ther 47:181–202.

Costall B, Domeney AM, Kelly ME, Tomkins DM, Naylor RJ, Wong EH, Smith WL, Whiting RL, Eglen RM (1993) The effect of the 5-HT_3 receptor antagonist, RS-4258-197, in animal models of anxiety. Eur J Pharmacol 234:91–99.

Derkach V, Surprenant A, North RA (1989) 5-HT_3 receptors are membrane ion channels. Nature 33:706–709.

Dunkley PR, Heath JW, Harrison SM, Jarvie PE, Glenfield PJ, Rostas JA (1988) A rapid Percoll gradient procedure for isolation of synaptosomes directly from an S1 fraction: homogeneity and morphology of subcellular fractions. Brain Res 441:59–71.

Edwards FA, Konnerth A, Sakmann B, Takahashi T (1989) A thin slice preparation for patch clamp recordings from neurones of the mammalian central nervous system. Pflugers Arch 414:600–612.

Fernandez-Chacon R, Konigstorfer A, Gerber SH, Garcia J, Matos MF, Stevens CF, Brose N, Rizo J, Rosenmund C, Sudhof TC (2001) Synaptotagmin I functions as a calcium regulator of release probability. Nature 410:41–49.

Forbush B (1984) An apparatus for rapid kinetic analysis of isotopic efflux from membrane vesicles and of ligand dissociation from membrane proteins. Anal Biochem 140:495–505.

Freund TF, Buzsáki G (1996) Interneurons of the hippocampus. Hippocampus 6:345–470.

Goodman LA (1954) Kolmogorov-Smirnov tests for psychological research. Psychol Bull 51:160–168.

Gulyás AI, Acsády L, Freund TF (1999) Structural basis of the cholinergic and serotonergic neurons in the hippocampus. Neurochem Int 34:359–372.

Katsurabayashi S, Kubota H, Tokutomi N, Akaike N (2003) A distinct distribution of functional presynaptic 5-HT receptor subtypes on GABAergic nerve terminals projecting to single hippocampal CA1 pyramidal neurons. Neuropharmacology 44:1022–1030.

Kawa K (1994) Distribution and functional properties of 5-HT_3 receptors in the rat hippocampal dentate gyrus: a patch clamp study. J Neurophysiol 71:1935–1947.

Koyama S, Kubo C, Rhee J-S, Akaike N (1999) Presynaptic serotonergic inhibition of GABAergic synaptic transmission in mechanically dissociated rat basolateral amygdala neurons. J Physiol 518:525–538.

Koyama S, Matsumoto N, Kubo C, Akaike N (2000) Presynaptic 5-HT3 receptor-mediated modulation of synaptic GABA release in the mechanically dissociated rat amygdala neurons. J Physiol 529: 373–383.

Koyama S, Matsumoto N, Murakami N, Kubo C, Nabekura J, Akaike N (2002) Role of 5-HT1A and 5-HT3 receptors in modulation of

synaptic GABA transmission in dissociated rat basolateral amygdala neurons. Life Sci 72:375–387.

Laporte AM, Koscielniak T, Ponchant M, Verge D, Hamon M, Gozlan H (1992) Quantitative autoradiographic mapping of 5-HT_3 receptors in the rat CNS using [^{125}I]iodo-zacopride and [^{3}H]zacopride as radioligands. Synapse 10:271–281.

Luebke JI, Dunlap K, Turner TJ (1993) Multiple calcium channel types control glutamatergic synaptic transmission in the hippocampus. Neuron 11:895–902.

Luebke JI, Greene RW, Semba K, Kamondi A, McCarley RW, Reiner PB (1992) Serotonin hyperpolarizes cholinergic low threshold burst neurons in the rat laterodorsal tegmental nucleus in vitro. Proc Natl Acad Sci USA 89:743–747.

Luebke JI, St. John J, Galler JR (2000) Prenatal protein malnutrition results in increased frequency of miniature inhibitory synaptic currents in rat CA1 pyramidal cells. Synapse 37:23–31.

Marek GJ, Aghajanian GK (1998) The electrophysiology of prefrontal serotonin systems: therapeutic implications for mood and psychosis. Biol Psych 44:1118–1127.

Maricq AV, Peterson AS, Brake AJ, Myers RM, Julius D (1991) Primary structure and functional expression of the 5HT_3 receptor, a serotonin-gated ion channel. Science 254:432–437.

McMahon LL, Kauer JA (1997) Hippocampal interneurons are excited via serotonin-gated ion channels. J Neurophysiol 78:2493–2502.

Miettinen R, Freund TF (1992a) Neuropeptide Y-containing interneurons in the hippocampus receive synaptic input from median raphe and GABAergic septal afferents. Neuropeptides 22:185–193.

Miettinen R, Freund TF (1992b) Convergence and segregation of septal and median raphe inputs onto different subsets of hippocampal inhibitory interneurons. Brain Res 594:263–272.

Morales M, Bloom FE (1997) The 5-HT_3 receptor is present in different subpopulations of GABAergic neurons in the rat telencephalon. J Neurosci 17:3157–3167.

Nayak SV, Ronde P, Spier AD, Lummis SC, Nichols RA (1999) Calcium changes induced by presynaptic 5-hydroxytryptamine-3 serotonin receptors on isolated terminals from various regions of the rat brain. Neuroscience 91:107–117.

Nevins ME, Anthony EW (1994) Antagonists at the serotonin-3 receptor can reduce the fear potentiated startle response in the rat: evidence for different types of anxiolytic activity? J Pharmacol Exp Ther 268:248–254.

Nichols RA, Mollard P (1996) Direct observation of serotonin 5-HT_3 receptor-induced increases in calcium levels in individual brain terminals. J Neurochem 67:581–592.

Papp EC, Hájos N, Acsády L, Freund TF (1999) Medial septal and median raphe innervation of vasoactive intestinal polypeptide containing interneurons in the hippocampus. Neuroscience 90:369–382.

Paudice P, Raiteri M (1991) Cholecystokinin release mediated by 5-HT_3 receptors in rat cerebral cortex and nucleus accumbens. Br J Pharmacol 103:1790–1794.

Piguet P, Galvan M (1994) Transient and long-lasting action of 5-HT on rat dentate gyrus neurones in vitro. J Physiol 481:629–639.

Ronde P, Nichols RA (1998) High calcium permeability of serotonin 5-HT_3 receptors on presynaptic nerve terminals from rat striatum. J Neurochem 70:1094–1103.

Ropert N, Guy N (1991) Serotonin facilitates GABAergic transmission in the CA1 region of rat hippocampus in vitro. J Physiol 441:121–136.

Rosenmund C, Stevens CF (1996) Definition of the readily releasable pool of vesicles at hippocampal synapses. Neuron 16:1197–1207.

Sakaba T, Neher E (2001) Calmodulin mediates rapid recruitment of fast-releasing synaptic vesicles at a calyx-type synapse. Neuron 32:1119–1131.

Schmitz D, Empson R, Heinemann U (1995) Serotonin reduces inhibition via 5-HT1A receptors in area CA1 of rat hippocampal slices in vitro. J Neurosci 15:7217–7225.

Shen R-Y, Andrade R (1998) 5-Hydroxytryptamine$_2$ receptor facilitates GABAergic neurotransmission in rat hippocampus. J Pharm Exp Ther 285:805–812.

Smith C, Moser T, Xu T, Neher E (1998) Cytosolic Ca^{2+} acts by two separate pathways to modulate the supply of release-competent vesicles in chromaffin cells. Neuron 20:1243–1253.

Stevens CF, Sullivan JM (1998) Regulation of the readily releasable vesicle pool by protein kinase C. Neuron 21:885–893.

Stevens CF, Wesseling JF (1998) Activity-dependent modulation of the rate at which synaptic vesicles become available to undergo exocytosis. Neuron 21:415–424.

St. John J, Rosene DL, Luebke JI (1997) Morphology and electrophysiology of dentate granule cells in the rhesus monkey: a comparison with the rat. J Comp Neurol 387:136–147.

Turner, TJ (2004) Nicotine enhancement of dopamine release by a calcium-dependent increase in the size of the readily-releasable pool of synaptic vesicles. J Neurosci, in press.

Turner TJ, Dunlap K (1995a) Pharmacological characterization of presynaptic calcium channels using subsecond biochemical measurements of synaptosomal neurosecretion. Neuropharmacology 34:1469–1478.

Turner TJ, Dunlap K (1995b) Prolonged time course of glutamate release from nerve terminals: relationship between stimulus duration and the secretory event. J Neurochem 64:2022–2033.

Turner TJ, Pearce LB, Goldin SM (1989) A superfusion system designed to measure release of radiolabeled neurotransmitters on a subsecond time scale. Anal Biochem 178:8–16.

Waeber C, Dixon K, Hoyer D, Palacios JM (1988) Localization by autoradiography of neuronal 5-HT_3 receptors in the mouse CNS. Eur J Neurosci 151:351–352.

Yakel JL, Jackson MB (1988) 5-HT_3 receptors mediate rapid responses in cultured hippocampus and a clonal cell line. Neuron 1:615–621.

(Accepted 4 August 2004)
(Available online 7 October 2004)